ARTICLE

Identification and circumvention of bottlenecks in CYP21A2-mediated premedrol production using recombinant *Escherichia coli*

Lisa König[1] | Simone Brixius-Anderko[1] | Mohammed Milhim[1] |
Daniela Tavouli-Abbas[1] | Michael C. Hutter[2] | Frank Hannemann[1] | Rita Bernhardt[1]

[1]Department of Biochemistry, Saarland University, Saarbrücken, Germany

[2]Center for Bioinformatics, Saarland University, Saarbrücken, Germany

Correspondence
F. Hannemann and R. Bernhardt, Department of Biochemistry, Saarland University, Campus B 2.2, 66123 Saarbrücken, Germany.
Email: f.hannemann@mx.uni-saarland.de
(F. H.) and ritabern@mx.uni-saarland.de (R. B.)

Present address
Simone Brixius-Anderko, College of Pharmacy, Department of Medicinal Chemistry, 428 Church St, University of Michigan, Ann Arbor, MI 48109.

Abstract

Synthetic glucocorticoids such as methylprednisolone are compounds of fundamental interest to the pharmaceutical industry as their modifications within the sterane scaffold lead to higher inflammatory potency and reduced side effects compared with their parent compound cortisol. In methylprednisolone production, the complex chemical hydroxylation of its precursor medrane in position C21 exhibits poor stereo- and regioselectivity making the process unprofitable and unsustainable. By contrast, the use of a recombinant *E. coli* system has recently shown high suitability and efficiency. In this study, we aim to overcome limitations in this biotechnological medrane conversion yielding the essential methylprednisolone-precursor premedrol by optimizing the CYP21A2-based whole-cell system on a laboratory scale. We successfully improved the whole-cell process in terms of premedrol production by (a) improving the electron supply to CYP21A2; here we use the N-terminally truncated version of the bovine NADPH-dependent cytochrome P450 reductase ($bCPR_{-27}$) and coexpression of microsomal cytochrome b_5; (b) enhancing substrate access to the heme by modification of the CYP21A2 substrate access channel; and (c) circumventing substrate inhibition which is presumed to be the main limiting factor of the presented system by developing an improved fed-batch protocol. By overcoming the presented limitations in whole-cell biotransformation, we were able to achieve a more than 100% improvement over the next best system under equal conditions resulting in $691 \, \text{mg·L}^{-1}\text{·d}^{-1}$ premedrol.

KEYWORDS
C21 hydroxylation, CYP21A2, cytochrome b_5, enzyme engineering, whole-cell biotransformation

1 | INTRODUCTION

Synthetic glucocorticoids are often used as immunosuppressants or for hormone replacement therapy compensating enzymatic disorders or deficiencies to treat various diseases like rheumatoid arthritis (Kadmiel & Cidlowski, 2013; McMaster & Ray, 2008). They are very similar to physiologically produced steroids, whereas their structure differs in additional functional groups such as hydroxy or methyl groups. These changes in the steroid framework modify the physiological properties such as solubility, skin or intestinal absorption, or steroid receptor affinity (Diederich et al., 2015). The latter particularly influences the suitability of the active substance for targeted medication, as natural glucocorticoids often cause unwanted side effects that typically manifest themselves in hypertension, hypokalemia, osteoporosis, and other symptoms (Henzen, 2003; Schäcke, 2002; Schäcke et al., 2004). These occur due to the

high coaffinity of these glucocorticoidal ligands to the mineralocorticoid receptor (MR) causing an aldosterone-like response (Farman & Rafestin-Oblin, 2017). Avoiding such side effects while increasing the therapeutic effect of steroidal drugs is a realistic goal and is often achieved by steroid modification. This can be illustrated particularly well using the example of the synthetic glucocorticoid methylprednisolone, which exhibits reduced MR affinity and multiplied glucocorticoid potency compared with its unmethylated derivative, prednisolone. Methylprednisolone, also known as medrol, is applied for the treatment of arthritis and other inflammatory diseases and thus, highly appreciated by the pharmaceutical industry (Bavetta, Bekhor, Shah, O'Day, & Nimni, 1962). The increasing demand of this compound requires the development of production strategies, that are aimed at achieving high-product yields while maintaining the cost-effectiveness of the process. Besides that, there is a common interest in reducing the ecological footprint to a minimum. The synthesis of this compound is challenging since, in particular, the introduction of a hydroxyl group in position C21 is a demanding step and difficult to achieve by chemical methods. Such reactions often require multistep processes involving the introduction of protective groups and the use of toxic reagents such as halogens. In addition, by-products increase the total expenditure and thus reduce production efficiency due to required purification by chromatographic methods (Koechlin, Kritchevsky, & Gallagher, 1951). The replacement of chemical by biotechnological processes has therefore aroused interest in recent decades, as the latter are highly suitable for the environmentally sustainable and economic production of pharmaceuticals. Bacterial fermentation for the production of pharmaceuticals offers (a) the possibility to accumulate high amounts of biomass by the use of simple and nontoxic raw materials, (b) a high-yield production of catalytically active enzymes and (c) the production of whole cells acting as biocatalysts. The latter can be used for the execution of regio- and stereospecific reactions under mild conditions while the cells provide and regenerate expensive cofactors such as NADPH (Bureik & Bernhardt, 2007). In particular, the use of cytochrome P450 enzymes (P450) in optimized bacterial whole-cell systems shows high potential and suitability for pharmaceutical production (Bernhardt, 2006; Urlacher & Girhard, 2012). Recently, the C21 hydroxylation of medrane has been established in a recombinant *Escherichia coli* (*E. coli*) whole-cell system that enables the CYP21A2-mediated production of premedrol, the precursor of methylprednisolone (Brixius-Anderko, Schiffer, Hannemann, Janocha, & Bernhardt, 2015). Although this system allows the production of considerable quantities of this compound, there is still potential for improvement by circumventing existing limitations of the CYP21A2-mediated conversion. Frequently observed bottlenecks of P450 systems include an insufficient electron delivery (Bernhardt & Urlacher, 2014; Sagadin, Riehm, Milhim, Hutter, & Bernhardt, 2018), whose efficiency is dependent on the choice of redox partners for bioconversion. Their suitability varies dependent on the respective P450 isoform. Additionally, there is evidence that the rate-limiting transfer of the second electron can be supported by an alternative bypass-pathway via cytochrome b_5, affecting product

formation velocity and efficiency (Vergères & Waskell, 1995). Another possible limitation that can occur in recombinant whole-cell biocatalysis is the molecular obstruction of substrate access to the active site (Wade, Winn, Schlichting, & Sudarko, 2004), which can be modulated by substitution of the relevant residues that cause steric or polar constraints. There is also the possibility of the substrate and product inhibition (Edwards, 1970; Lin et al., 2001), caused by exposure of toxic substrates or complex-formation of the enzyme with the substrate or product at excessively high concentrations, respectively. Here, we addressed all of these possible obstacles and, thus, (a) improved the efficiency of electron supply by using the modified natural redox partner $bCPR_{-27}$ and the coexpression of cytochrome b_5, (b) improved substrate conversion by molecular modification of the substrate access channel, and (c) bypassed substrate or product inhibition by performing fed-batch cultivation of *E. coli*.

2 | MATERIALS AND METHODS

2.1 | Chemicals and enzymes

Medrane and premedrol were obtained from Sanofi, Frankfurt-Höchst (DE) and of highest purity. Restriction enzymes were obtained from New England Biolabs (Ipswich, MA) and Fast-Link™ Ligase was purchased from Lucigen Corporation. The PCRs were performed with Phusion® High-Fidelity DNA Polymerase and dNTP's, both obtained from New England Biolabs (Ipswich, MA). Further chemicals and reagents were purchased from standard resources and are of highest purity.

2.2 | Bacterial strains and cultivation

All cloning experiments were performed with *E. coli* strain TOP10 (Invitrogen). Protein synthesis and whole-cell biotransformation were carried out in the *E. coli* strain C43(DE3) as described in (Miroux & Walker, 1996). Transformed cells were stored as glycerol stock with a 1:1 mixture of an overnight culture and glycerol (80%) at −80°C.

2.3 | Plasmid construction and mutagenesis

2.3.1 | CYP21A2 and CPR_{-27} expression

The bovine CYP21A2 [UniProt ID: P00191; PDB code: 3QZ1] and CPR_{-27} [UniProt ID: Q3SYT8] were expressed in C43(DE) while the latter is an N-terminally truncated version with a C-terminal 3-glycine-6-histidine tag as described (Neunzig et al., 2014). The truncation of 27 amino acids at the N-terminus enables high-yield expression of a soluble catalytically active CPR. The cloning and generation of the vector p21b_bRED(−27) was performed as described in (Brixius-Anderko et al., 2015; Neunzig et al., 2017) (Figure 1a).
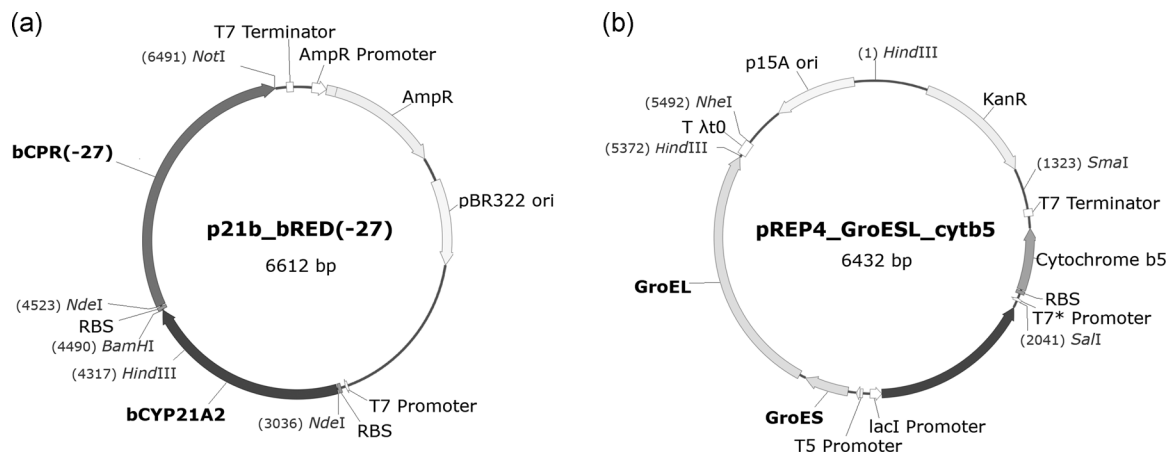
FIGURE 1 Vector maps containing genes for CYP21A2, CPR, cytochrome b_5, and chaperonins. Restriction enzyme cleaving sites are depicted in red with corresponding positions in the respective plasmid. (a) Vector map of bicistronic p21b_bRED(− 27) containing the genes of the bovine CYP21A2 and N-terminally truncated bovine CPR (CPR$_{−27}$) with the corresponding ribosome binding sites (RBS). Expression of these proteins is regulated by the T7 promoter. The plasmid contains the gene for ampicillin resistance (AmpR) and a pBR322 origin of replication (ori). (b) Vector map of the plasmid pREP-groESL_cytb5, a modified derivative of pREP4-groESL (Cole, 1996) containing the additional gene of cytochrome b_5 with corresponding RBS under control of a modified T7 promoter (T7*) with decreased induction strength (Ikeda et al., 1992) and the gene for kanamycin resistance (KanR)

2.3.2 | Cytochrome b_5 and GroEL, GroES chaperonins

The vector pREP4-groESL_cytb5 (Figure 1b) was generated using the pREP4-groESL backbone (Cole, 1996). For cloning of the bovine cytochrome b_5 [UniProt ID: P00171], the expression cassette SmaI-P$_{T7mod}$-cytochrome b_5-T$_{T7mod}$-SalI was amplified via PCR using the template previously described (Klymiuk et al., 2017) and primers listed in Table S1. The T7 promoter sequence was modified (P$_{T7mod}$), to reduce the cytochrome b_5 expression level. Hence, adenine was substituted into thymine in position −6 of the T7 sequence as proposed by Ikeda, Ligman, and Warshamana (1992). Following, the digested amplicon was inserted into SmaI and SalI treated pREP4-groESL via ligation.

2.3.3 | Site-directed mutagenesis in M210 of CYP21A2

p21b_bRED(−27) served as a template for a Quik change® mutagenesis changing position M210 of the bovine CYP21A2 sequence. For this, Pfu polymerase was used and mutagenesis was performed according to manual instructions from Agilent Technologies (Santa Clara, CA). All utilized primers are listed in Table S1.

2.4 | Purification of CYP21A2, cytochrome b_5, and CPR$_{−27}$ and in vitro conversion of medrane

Expression and purification of the bovine proteins CYP21A2, CPR$_{−27}$, and cytochrome b_5 were performed as described before (Brixius-Anderko et al., 2015; Neunzig et al., 2014; Schiffer et al., 2016).

Aliquots were stored at −80°C until used. Protein concentration of bCPR$_{−27}$ was calculated using a molar extinction coefficient $\varepsilon_{585} = 2.4\,\text{mM}^{-1}\cdot\text{cm}^{-1}$ (Vermillion, Janice, & Coon, 1978). The concentration of bovine cytochrome b_5 was determined using a difference extinction coefficient of $185\,\text{mM}^{-1}\cdot\text{cm}^{-1}$ for the absorbance change at 424–409 nm (Mulrooney & Waskell, 2000). CYP21A2 concentration was determined by performing difference spectroscopy according to Omura and Sato using a molar extinction coefficient of $\varepsilon_{448} = 91\,\text{mM}^{-1}\cdot\text{cm}^{-1}$ (Omura & Sato, 1964). The determination of reaction velocity dependent on enzyme ratio were performed using the purified enzymes in a reconstituted in vitro system. The reaction was carried out in 250 µl reaction buffer containing potassium phosphate buffer (KP$_i$ buffer) [50 mM K$_2$HPO$_4$/KH$_2$PO$_4$; pH 7.4], 1 mM MgCl$_2$, 5 mM glucose-6-phosphate and 1 U glucose-6-phosphate dehydrogenase. Purified bCYP21A2 (0.5 µM) and varying concentrations of the CPR$_{−27}$, cytochrome b_5 and medrane were added to the reaction buffer. The reaction was started by application of 500 µM NADPH into the prewarmed reaction mixture, followed by incubation at 37°C for a defined time. The reaction was stopped by addition of 250 µl of chloroform.

2.5 | Steroid quantification by reverse-phase high-performance liquid chromatography (RP-HPLC)

For product quantification via RP-HPLC, the samples were extracted twice with double volumes of chloroform. The organic solvent was evaporated and the remaining steroids were suspended in 50% acetonitrile and separated on a Jasco reverse phase HPLC system of the LV2000 and LV900 series using a reverse-phase ec MN NucleoDur C18 (4.0 × 125 mm; Macherey-Nagel, Betlehem, PA). The column was kept at an oven temperature of 40°C. For measurements of the samples

an acetonitrile/water gradient was applied with a flow rate of 0.8 ml/ min and absorbance of the substances was detected at a wavelength of 240 nm (Solution A: 50% ACN; Solution B: 100% ACN; 0–8 min: 100% A; 8–10 min: 10% A; 10–10.1 min 100% A, 10.1–15 min 100% A). The retention times of medrane (3.2 min) and premedrol (2.2 min) were verified with the respective standards. The relative peak area of each substance was used for calculation of the conversion rates and product concentration.

2.6 | Protein expression and whole-cell biocatalysis

Expression of CYP21A2 and redox partners was performed by inoculation of LB medium with glycerol stocks from transformed C43(DE3) *E. coli* cells with the vectors p21b_bRED(−27) (Figure 1a) or p21b_ArEt (Brixius-Anderko et al., 2015) and pGro12 (Nishihara, Kanemori, Kitagawa, & Yura, 1998) or pREP-groESL_b5 (Figure 1b). The seed culture was incubated at 37°C overnight. The main culture was generated in 300 ml baffled flasks by inoculation of 30 ml of terrific broth (TB) medium containing the respective antibiotics (100 µg/ml ampicillin and 50 µg/ml kanamycin) inoculated with the seed culture using a ratio of 1:100. When the $OD_{600\,nm}$ reached 0.5, the protein production was induced by the addition of 4 g L^{-1} arabinose, 1 mM isopropyl-β-D-thiogalactoside (IPTG) and 1 mM δ-aminolevulinic acid. The temperature was reduced to 30°C and the expression was performed for 24 hr at 150 rpm. After the expression period, the cells were harvested by centrifugation (2500 g, RT, 15 min) and washed with 50 mM KP_i. After the second centrifugation, the pellet was suspended in 50 mM KP_i adjusting cell densities of 24–96 g wet cell weight (g_{wcw})/L. The biotransformations were performed in 100 ml baffled flasks containing 10 ml of the culture unless otherwise stated. Polymyxin B (32.5 µg/ml) was added for cell permeabilization providing an improved substrate uptake (Janocha & Bernhardt, 2013). Biotransformations using batch cultivation were performed by the addition of 1.2 or 4.8 mM medrane and 2% or 8% (vol/vol) glycerol. Fed-batch fermentation was carried out by adding 1.2 mM medrane and 2% (vol/vol) glycerol, which was repeated for three times in 2 hr periods. Medrane conversions were performed at 30°C and 150 rpm for a defined time. The steroid substrate was dissolved in dimethyl sulfoxide, which did not exceed 4.8% in conversion cultures. The reaction was stopped by the addition of the double volume of chloroform.

2.7 | Computational methods

The crystal structure of the bovine CYP21 (PDB 3QZ1) was used as a receptor for docking into the wild-type, whereas the M210V mutant was constructed using the SWISS pdb viewer (version 4.0.1) (Guex & Peitsch, 1997). For the necessary preparation steps before docking AutoDock Tools (Windows version 1.5.6r3) was used (Sanner, 1999). AMBER charges were assigned to the amino acids of the protein part and Gasteiger-Marsili charges were computed for the heme cofactor.

To account for its oxidation state, the partial charges were adjusted to 0.400e on the iron atom and –0.348e to each of its ligating nitrogen atoms, respectively. The rectangular grid box (56 × 50 × 64) was centered around residue 210 To capture all conceivable binding positions of the ligands in this region. The grid spacing was set to the default value of 0.375 Å. Medrane and 17α-hydroxyprogesterone (17OHP) were constructed manually and energetically optimized using the MM+ force field parameters as implemented in HYPERCHEM (HYPERCHEM, Version 6.02, Hypercube Inc., Gainsville, FL). Atom types and Gasteiger-Marsili charges for use in AutoDock (version 4.2) (Huey, Morris, Olson, & Goodsell, 2007; Morris et al., 1998) were computed with in-house PERL scripts. During docking all rotatable bonds of the ligands were treated as flexible, whereas the protein part was kept rigid. A total of 250 runs of the Lamarckian Genetic Algorithm for each ligand were carried out, otherwise default parameters of AutoDock were applied. Hydrophobicity profiles of the full-length and truncated bCPR were determined and compared using the ExPASy online tool Protscale (Gasteiger et al., 2005) based on the amino acid scale of Kyte and Doolittle (1982).
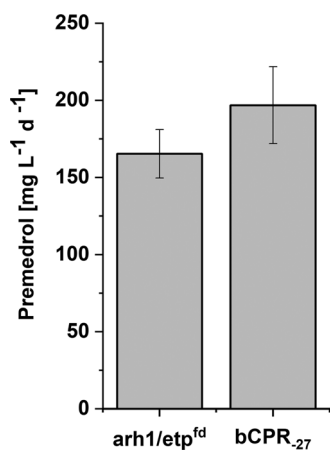
3 | RESULTS AND DISCUSSION

3.1 | In vivo effect of the N-terminal CPR truncation on premedrol formation in the *E. coli* whole-cell system

To enhance the previously established whole-cell system in *E. coli* C43(DE3) (Brixius-Anderko et al., 2015), we considered different aspects frequently limiting the efficiency of whole-cell biotransformations. The hydroxylating activity of bovine CYP21A2 depends on the coexistence of a suitable redox partner that mediates the transfer of two electrons from $NADPH^+$ to CYP21A2. This event enables the enzymatic regioselective oxidation of medrane in C21 resulting in premedrol. Since an optimal electron supply is allocated to be an important factor in limiting the conversion yield of P450 mediated systems, we sought to optimize this by substitution of the coexpressed redox partner in the *E. coli* whole-cell system. Therefore, we modified the membrane-bound microsomal bovine CPR, which is the naturally occurring redox partner of bovine CYP21A2. According to a previous study, the N-terminal truncation of 27 amino acids (−27) of the human CPR led to an improved solubility and higher protein concentrations without affecting the enzyme's activity in a recombinant *E. coli* system (Sandee & Miller, 2011). For electron transfer, positively charged residues on the proximal site of CYP21A2 are interacting with acidic residues on the CPR surface (Hlavica, Schulze, & Lewis, 2003; Shen, Porter, Wilson, & Kasper, 1989). Since the removal of 27 N-terminal amino acids did not affect catalytic activity (Sandee & Miller, 2011), the binding sites should be unaffected. To this end, we generated a modified version of the plasmid p21b_bRED (Brixius-Anderko et al., 2015), harboring the encoding sequence of bCPR−27. The truncated protein-enhanced medrane conversion in whole-cell biotransformations by about 19%

compared with the reported arh1/etp^{fd} based redox system resulting in 196.8 ± 24.9 mg·L^{-1}·d^{-1} although statistical significance cannot be assured (Figure 2). The presented premedrol production here did not exceed 320 mg L^{-1} as observed by Brixius-Anderko et al. using arh1/etp^{fd}, since the latter yield was obtained by multiple addition of lower substrate concentrations summed up to 1 mM. However, comparing premedrol production obtained by non-successive substrate addition, using the bCPR$_{-27}$ increased the premedrol production 2.4-fold compared with premedrol production supported by WT CPR (Brixius-Anderko et al., 2015).

This difference in efficiency is due to the membrane-bound nature of the WT microsomal CPR which makes it difficult to be overexpressed in a recombinant bacterial system. The removal of the N-terminal membrane-binding domain putatively increased the protein's solubility, as this region is described to be hydrophobic in rat (Gilep, Guryev, Usanov, & Estabrook, 2001), yeast (Venkateswarlu, Lamb, Kelly, Manning, & Kelly, 1998), human (Migita, Togashi, Minakawa, Zhang, & Yoshida, 2005) and rabbit (Masters, 2005) CPR. Additionally, in silico determination of hydrophobicity profiles and average hydrophobicity indices of the bovine CPR sequence revealed that the truncation of the N-terminus decreased hydrophobicity of the protein by 2.7%. This could result in increased stability and, therefore, higher expression level in the recombinant host. With this, the excessive accumulation and degradation of hydrophobic proteins in the cytoplasm is prevented. Consequently, this facilitated the presence of higher quantities of catalytically active protein. Additional in vitro experiments using different ratios of P450:CPR revealed that the increase of CPR up to 1:4 leads to an increase in reaction velocity (Figures S1 and 3) forming premedrol. Based on this
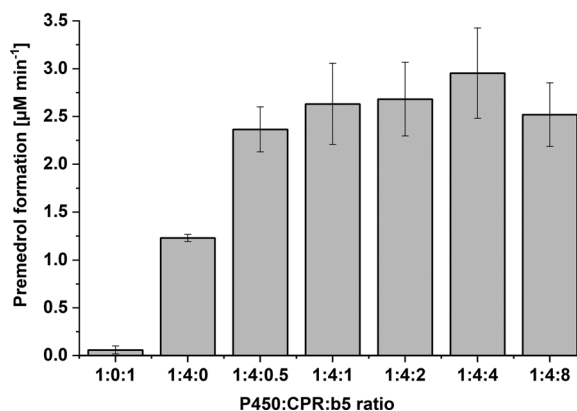
observation, bCPR$_{-27}$ was consecutively used for all subsequent experiments.

3.2 | In vitro effect of cytochrome b_5 on premedrol formation

As shown before by using a truncated CPR version, the efficiency of electron transfer is one of several limiting factors on whole-cell medrane conversions in recombinant *E. coli* (Figure 2). Thus, we sought to introduce a putatively supporting protein that is able to interact with the CPR and/or CYP21A2. In microsomes, cytochrome b_5 is colocated with CYP21A2 and CPR and has previously been shown to support several individual P450s in their reaction efficiency, for instance, CYP3A4, CYP2B4 and CYP17A1 (Bart & Scott, 2017; Bridges et al., 1998; Gilep et al., 2001; Katagiri, Kagawa, & Waterman, 1995). However, the supportive effect is dependent on the individual P450 isoform as well as the corresponding redox partner and the molar ratio of the present enzymes (Imai & Sato, 1977; Lu, West, Vore, Ryan, & Levin, 1974; Morgan & Coon, 1984; Schenkman, Jansson, & Robie-Suh, 1976).

The mechanism of cytochrome b_5 action is hypothesized as follows: (a) allosteric activation of P450 supporting the correct positioning towards CPR (Miller, 2005), (b) cytochrome b_5 acts as an electron transfer intermediate between the reductase and P450s. Whereas the CPR transfers the first electron with high efficiency, cytochrome b_5 provides the rate-limiting input of the second electron to P450 (Schenkman & Jansson, 2003), (c) complexation of cytochrome b_5 to P450 leading to a stabilization of the oxycytochrome P450 complex. In this way, cytochrome b_5 can provide a faster transfer of the second electron than the formation and release of a superoxide anion. The three suggested mechanisms allow the


FIGURE 2 CYP21A2-mediated whole-cell conversion of medrane in dependence on the redox partners (arh1/etp^{fd}; bCPR$_{-27}$). The 24 hr expression took place in TB medium after induction with 1 mM IPTG, δ-ALA, and 0.4% arabinose. The reactions were carried out in 30 ml of KPi (pH 7.4), containing 30 μg/ml polymyxin B, 2% glycerol, 1 mM medrane, and 24 g$_{wcw}$/L of recombinant *Escherichia coli* cells for 24 hr. Extracted steroids were quantified via RP-HPLC. Values represent the mean of three conversion experiments. Error bars indicate respective standard deviations. IPTG, isopropyl-β-D-thiogalactoside; RP-HPLC, reverse-phase high-performance liquid chromatography; δ-ALA, δ-aminolevulinic acid

FIGURE 3 Time-dependent in vitro conversion of medrane to its 21-hydroxylated product, premedrol, in dependence on the CYP21A2:CPR:cytochrome b_5 ratio. The in vitro conversions of 100 μM medrane were performed utilizing purified bCYP21A2, bCPR$_{-27}$ and cytochrome b_5 in KP$_i$ buffer. Independent samples were measured within the linear range (3, 5, 10, and 30 min) via RP-HPLC. Error bars indicate the respective standard deviation. b5: cytochrome b_5; CPR, CPR$_{-27}$; P450, CYP21A2; RP-HPLC, reverse-phase high-performance liquid chromatography

increase of product formation without influencing NADPH consumption (Gorsky & Coon, 1986; Gruenke, Konopka, Cadieu, & Waskell, 1995). To investigate the effect of cytochrome b_5 on CYP21A2 activity, we performed in vitro conversions of medrane using the purified bovine enzymes of CYP21A2, bCPR$_{-27}$ and cytochrome b_5 (Table S2) at varying ratios from 1:4:0 to 1:4:8 (Figure 3). The optimal P450:CPR ratio was previously determined to be 1:4, as shown in Figure S1. At a P450:CPR:cytochrome b_5 ratio of 1:0:1 no product was formed highlighting the mandatory role of CPR for CYP21A2 activity which increased up to 1.25 µM premedrol/min at a ratio of 1:4:0 (Figure 3). We observed that cytochrome b_5 has a supporting effect on product formation, which is increased at least by 90% at a ratio of 1:4:0.5 compared with 1:4:0 and did not alter considerably at higher P450:bCPR$_{-27}$:cytochrome b_5 ratios (Figure 3). The lack of premedrol production at ratio 1:0:1 confirmed the above-stated hypothesis that the electron transfer, at least the transfer of the first electron, is exclusively mediated by CPR and cannot be replaced by cytochrome b_5 (Miller, 2005; Schenkman & Jansson, 2003). The enhancing effect of the cytochrome b_5 at ratios of 1:4:0.5 and above shows that despite the removal of the first 27 amino acids of the CPR protein sequence, interaction between both, CPR and cytochrome b_5, still is possible resulting in a higher reaction velocity. With regard to the elevating effect of cytochrome b_5 on the CYP21A2 related biotransformation, hypotheses (a)–(c) are conceivable in this context. By contrast, a previous study described an inhibitory effect of

cytochrome b_5 on the CYP21A2 activity in vitro (Wang et al., 2017). The opposite effect demonstrated there may, on one hand, be due to the use of enzymes from different sources. Whereas in our experiments all enzymes originate exclusively from the bovine species, in those experiments human CYP21A2, cytochrome b_5 and rat CPR were used. Moreover, different substrates were investigated (medrane and progesterone, respectively), which could affect the influence of cytochrome b_5 on the performance of P450 (Bart & Scott, 2017). Finally, in the experiments described by Wang et al. (2017), excessive concentrations of cytochrome b_5 (1:300) were used, which may lead to the contrary effect as observed in our studies, since we did not exceed a P450 to cytochrome b_5 ratio of 1:8.

3.3 | Protein engineering of bCYP21A2 via site-directed mutagenesis and in vivo screening

Another possible limiting factor in biotransformations is steric hindrance of the substrate access into the active site, preventing substrate-uptake or product release. Compared with the natural CYP21A2 substrate 17α-hydroxyprogesterone (17OHP) (Figures 4a and 4c) medrane possesses an additional methyl group in C6 and a hydroxy group in C11 (Figures 4b and 4d). Hence, modification of the substrate access channel could lead to higher efficiency in medrane
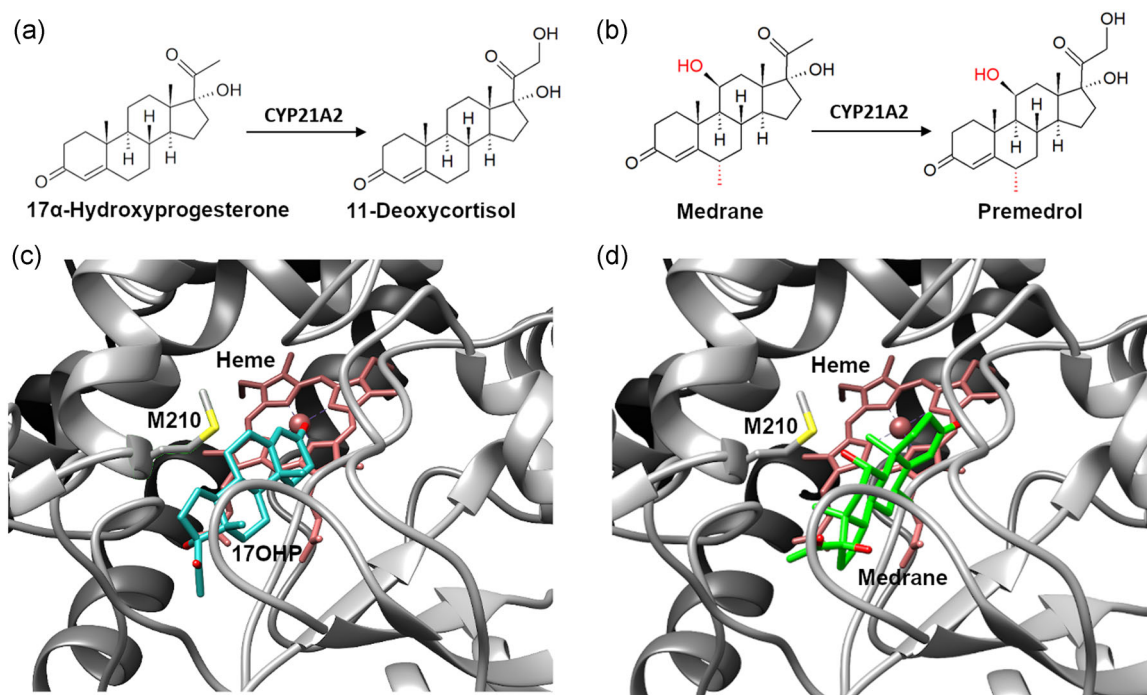

FIGURE 4 Scheme of the CYP21A2-catalyzed C21-hydroxylation and structure of the wild type (WT) CYP21A2 substrate access channel in the presence of 17α-hydroxyprogesterone (17OHP). (a) The natural substrate 17OHP is hydroxylated by CYP21A2 yielding 11-deoxycortisol. (b) The synthetic steroid medrane is hydroxylated at position C21 producing premedrol. Compared to 17OHP, medrane possesses an additional hydroxy group at C11 and a methyl group at C6 as depicted in red. (c, d) Top view on the CYP21A2 substrate access channel illustrating the location of methionine (position 210, sulfur colored in yellow) and the ligand. (c) 17OHP as being present in the X-ray protein structure of bovine CYP21A2 (PDB: 3QZ1 [marine sticks] (Zhao et al., 2012). (d) Obtained docking position of medrane (green sticks). Oxygen atoms of the steroidal structure are depicted in red, the prosthetic heme group in pink, and its iron atom as sphere [Color figure can be viewed at wileyonlinelibrary.com]

conversion. According to Zhao et al. (2012), the methionine in position 210 of bCYP21A2 is part of the distal 17OHP-binding region which interacts with the substrate within 4 Å and is located at the substrate access channel (Figure 4c). To enhance substrate access to the active site, we thus examined the impact of steric effects in product formation in vivo. To this end, we performed site-directed mutagenesis of M210 by introducing other hydrophobic residues of different size (valine, glycine, alanine, isoleucine and phenylalanine). Indeed, substitution with the smaller valine yielded a 1.3-fold increase in premedrol formation (Figure 5a), resulting in $255 \pm 20 \, \text{mg} \cdot \text{L}^{-1} \cdot 48 \, \text{hr}^{-1}$ (Figure 5b), whereas the introduction of smaller residues into position M210 produced premedrol levels not different from that of the WT (Figure 5a). We assume that steric and hydrophobic effects play a role in this context. Since valine is a more hydrophobic residue than methionine (Eisenberg, 1984; Kyte and Doolittle, 1982), hydrophobic interactions could be implicated to allow correct substrate orientation and faster guidance towards the catalytically active heme. Our docking results showed energetically preferred binding positions of both medrane and 17OHP in the same region as the ligand in the crystal structure (3QZ1), considering its limited resolution of 3 Å (see Figures 4c and 4d). Interestingly, the obtained docking conformations in the M210V mutant were identical to those in the wild type (data not shown). However, since residue 210 is not in direct contact with the ligands, the introduction of a smaller side chain (valine) obviously does not affect their binding position. Nevertheless, it is likely that conformational changes of the protein go along with the diffusion of the ligands further to the active site, which, however, cannot be elucidated by docking. Therefore, we assume that the smaller side chain in position 210 affects the dynamics of substrate access indirectly, for example by altered enzyme stability or expression level. However, it cannot be ruled out that the mutation may facilitates the substrate's access by conformational changes of the protein. Unfortunately, experiments analyzing modifications of the active site (M197 with saturation mutagenesis) or the surface (L442A and L224R) of CYP21A2 for altered solubility did not produce any improved variants for premedrol production (data not shown).

3.4 | Combinatorial application of developed strategies on whole-cell biotransformation of medrane

Although the effect of CPR truncation on premedrol production and CYP21A2 mutagenesis has been demonstrated in the *E. coli* whole-cell system, the effects of cytochrome b_5 copresence were so far shown only in vitro. This encouraged us to create a functional in vivo whole-cell system that combines the three optimization strategies. To keep the number of expression vectors to a limit of two, we created a vector containing the genes for the chaperonins GroES/EL and cytochrome b_5. For this purpose, we modified the vector pREP4-groESL (Cole, 1996) and introduced the gene for cytochrome b_5 under the control of a modified T7 promoter. As the P450:CPR: b_5 ratio 1:4:0.5 is sufficient to have an elevating impact on product formation in vitro (Figure 3) we introduced a point mutation into the T7 promoter according to Ikeda et al. (1992). This modification leads to a residual promoter activity of 13%, which prevents excessive cytochrome b_5 production and thus maintains efficient coexpression of bCPR$_{-27}$ and CYP21A2. *E. coli* C43(DE3) was cotransformed with the WT CYP21A2 (p21b_bRED(−27)) or modified CYP21A2
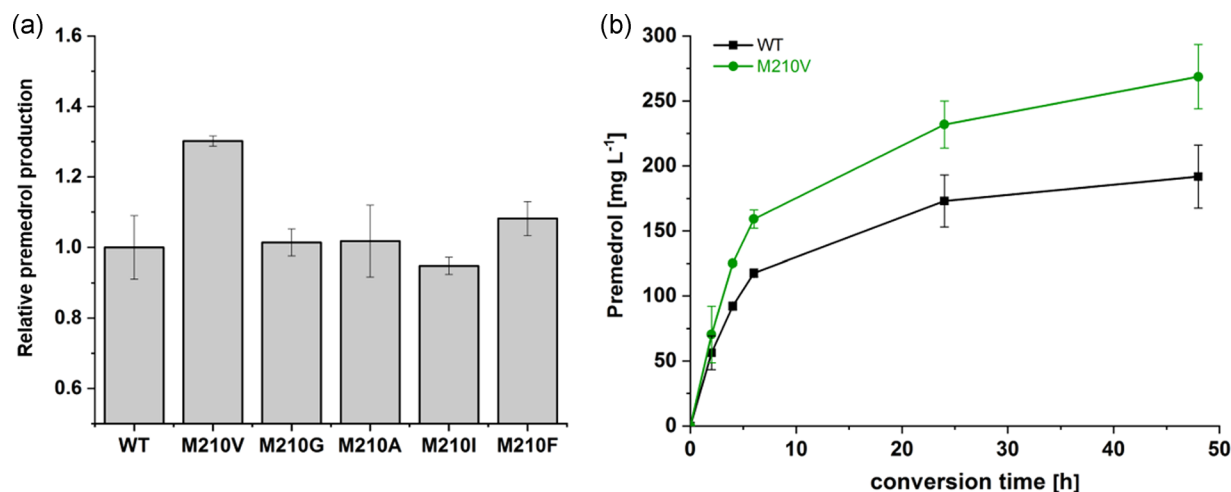
FIGURE 5 In vivo conversion of medrane dependent on replacements in position M210 of bCYP21A2. (a) Relative premedrol production standardized to the WT (M210). Premedrol concentrations were analyzed via RP-HPLC after a conversion period of 24 hr. (b) Absolute premedrol concentration dependent on the conversion time. The 24 hr expression period took place in TB medium after induction with 1 mM IPTG, δ-ALA, and 0.4% arabinose. The reactions were carried out in 30 ml of KPi (pH 7.4) containing 30 μg/ml polymyxin B, 2% glycerol, 1.2 mM medrane, and 24 g_{wcw}/L of recombinant *Escherichia coli* cells for 24 hr. Extracted steroids were quantified via RP-HPLC. Values represent the percentage mean of three conversion experiments. Error bars indicate the respective standard deviation. Values were normalized on premedrol productions of the WT. IPTG, isopropyl-β-D-thiogalactoside; RP-HPLC, reverse-phase high-performance liquid chromatography; TB, terrific broth; WT, wild type; δ-ALA, δ-aminolevulinic acid [Color figure can be viewed at wileyonlinelibrary.com]
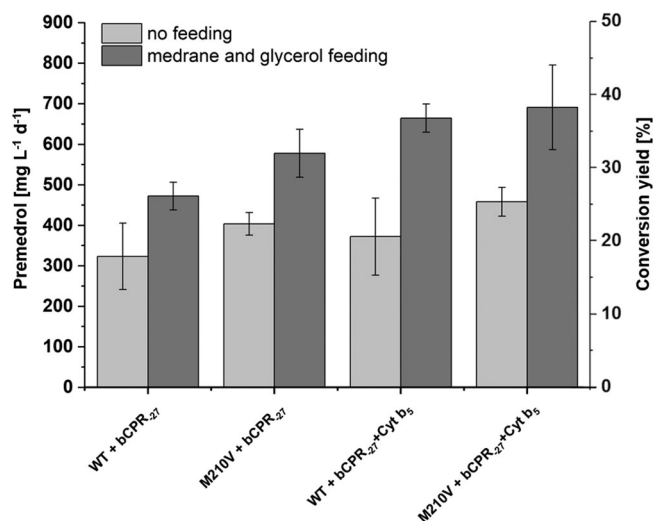
FIGURE 6 CYP21A2-mediated whole-cell conversion of medrane dependent on the CYP21A2 variant (WT or M210V) and the presence of cytochrome b_5 (Cyt b_5). The 24 hr expression period took place in TB medium after induction with 1 mM IPTG, δ-ALA and 0.4% arabinose. The reactions were carried out in 10 ml of KP$_i$ buffer (pH 7.4) for 24 hr, containing 32.5 µg/ml polymyxin B, 2% glycerol and 96 g$_{wcw}$/L of recombinant *Escherichia coli* cells. 4.8 mM of medrane was either added at the beginning of the conversion period (no feeding, bright columns) or stepwise in 2-hr time slots each with 1.2 mM medrane (t0-t6) and 2% glycerol (t$_2$-t$_6$) (feeding, dark columns). Extracted steroids were quantified via RP-HPLC. Values represent the mean of three conversion experiments. Error bars indicate respective standard deviations. IPTG, isopropyl-β-D-thiogalactoside; RP-HPLC, reverse-phase high-performance liquid chromatography; TB, terrific broth; δ-ALA, δ-aminolevulinic acid

containing vector (p21b_M210V_bRED(−27)) and with the chaperonin vector (pGro12) or chaperonins and cytochrome b_5 containing vector (pREP4-groESL_cytb5), respectively (Figure 1). Biotransformation was performed by adding 4.8 mM medrane (Figure 6, bright columns) and 8% (vol/vol) glycerol. In batch cultures (Figure 6, bright columns) the coexpression of cytochrome b_5 with WT CYP21A2 showed an elevating effect on premedrol production by 15% compared with cultures solely expressing WT CYP21A2. The substitution M210V in CYP21A2 yielded 404 ± 28 mg·L^{-1}·d^{-1}, corresponding to a 25% increased product formation compared with WT CYP21A2, which is in good agreement with the observations of the mutant screening shown above (Figure 5). The additional coexpression of cytochrome b_5 slightly increased premedrol formation by further 13%, summing up to 41% compared with WT CYP21A2 without cytochrome b_5 under batch-cultivation conditions. To investigate whether a possible substrate inhibition could be a bottleneck of the process encountered with high initial substrate concentrations, we changed the protocol from batch- into fed-batch cultivation. To this end, we applied 1.2 mM of the steroidal substrate medrane together with 2% glycerol in four consecutive feeding steps, every 2 hr (Figure 6, dark columns). Indeed, the successive addition of the substrates, medrane and glycerol, had an increasing effect on final premedrol concentrations as well as on the respective

conversion yields. The latter was enhanced by a maximum of 16% (WT CYP21A2 with coexpressed cytochrome b_5) when using fed-batch cultivation in comparison to the batch method.

The fed-batch method led to substantially higher product concentrations for both, the CYP21A2 WT and M210 mutant showing an enhancement by 46% and 43%, respectively, compared with respective premedrol concentrations resulted from batch cultivation (Figure 6, bright columns). This resulted in concentrations of 472 ± 34 (WT) and 578 ± 59 mg·L^{-1}·d^{-1} (M210V) (Figure 6, dark columns). The enhancing effect of the amino acid replacement M210V in CYP21A2 is reflected by an improvement of 22% in premedrol productivity in fed-batch cultivation, compared with the WT CYP21A2. This improvement corresponds to a final product concentration of 578 ± 59 mg·L^{-1}·d^{-1}. However, the enhancing effect of the mutation M210V seemed to be limited to 4% (691 ± 104 mg·L^{-1}·d^{-1}), when cytochrome b_5 is coexpressed compared with WT CYP21A2 coexpressed with cytochrome b_5 (664 ± 35 mg·L^{-1}·d^{-1}). The premedrol production is leveled off at 691 ± 104 mg·L^{-1}·d^{-1}. This indicates that there are still other aspects, limiting the process such as restricted substrate uptake or product release. Cultures coexpressing cytochrome b_5 show highest divergence between batch- and fed-batch induced premedrol productivity which correspond to an increase by 79% and 51% of the WT and M210V variant, respectively, compared with the respective batch induced premedrol productivity. The improved method led to final space-time yields of 665 ± 35 and 691 ± 104 mg·L^{-1}·d^{-1}, respectively. In fed-batch cultivation the coexpression of cytochrome b_5 results in an elevation of final premedrol concentrations by 40% when WT CYP21A2 is used and by 19% when mutant M210V is applied (compared with the respective fed-batch cultivation values without cytochrome b_5 coexpression). The latter reflects the maximum productivity and conversion yield obtained here by the optimized process.

Taken together, we showed that by successive substrate feeding we reduced inhibition encountered with high initial substrate concentrations. This effect was also observed under conditions, where the conversion yield decreases asymptotically with increasing substrate concentrations indicating a substrate-mediated inhibition of CYP21A2 (Figure S2). Lin et al. showed the same phenomenon for several P450 isoforms, and, thus, proposed a two-site model for understanding dose-depending substrate inhibition in P450-catalyzed reactions. They hypothesized that the substrate has high affinity to the active site and lower affinity to a second binding site, which is occupied at extensive concentrations of the substrate (Lin et al., 2001). This model can be helpful to describe the higher productivity by feeding experiments, where substrate concentrations are kept low due to continuous substrate consumption. In vivo, this mechanism could be used for a natural regulation process, since steroid metabolism is a sensitive, fine-tuned physiological system. Especially the activity of CYP21A2 is needed to be regulated for example by feedback-responses, as the C21 hydroxylation results in activation of the steroids to act as highly potent ligands of the glucocorticoid or MR (Attardi et al., 2007; Boland, 1961). Further, we

FIGURE 7 Summary of the milestones during optimization of the presented whole-cell system. The individual stages are visualized in chronological order showing their impact on premedrol production per 24 hr
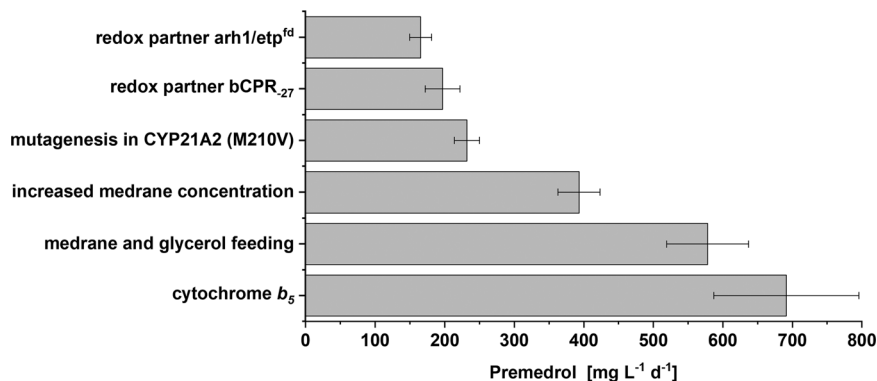
showed that the enhancing effects of the M210V mutation and cytochrome b_5 on CYP21A2 activity are recognizable more clearly under the conditions of fed-batch cultivation. Thus, we assume that the inhibitory effect, which is related to a high substrate concentration is a major limitation of the process. Further optimization to exploit the complete catalytic potential could be realized by controlled fermentation in an automated bioreactor, that allows continuous titration of the substrate, which is ideally matched on residual substrate concentration within the culture.

4 | CONCLUSION

We successfully optimized the CYP21A2-based whole-cell system in *E. coli*. The application of a truncated CPR and coexpression of cytochrome b_5 led to increased efficiency of premedrol formation putatively based on an improved electron supply or allosteric interaction (Figure 7). The amino acid replacement M210V located in the substrate access channel caused a slightly increased product formation. The visibility of the supportive optimizations was limited by single-step substrate application, which we finally uncovered by successive substrate feeding. Applying the enhanced fed-batch protocol together with the use of bCPR$_{-27}$ and CYP21A2_M210V as well as the coexpression of cytochrome b_5 enabled us to produce up to 691 mg·L^{-1}·d^{-1} premedrol within a biotechnological *E. coli* based whole-cell system which is a more than a 100% improvement compared with our previously reported system under similar conditions (Brixius-Anderko et al., 2015). This is a big step forward towards application of this system in an industrial process for the sustainable production of the methylprednisolone-precursor premedrol.

CONFLICT OF INTERESTS

The authors declare that there are no conflict of interests.

AUTHOR CONTRIBUTIONS

L. K. drafted the manuscript and performed in vivo experiments. S. B. A. participated in study design and manuscript drafting, created the M210 mutant library, performed in vivo experiments and purified CYP21A2. M. M. designed and established the truncated CPR-dependent whole-cell system, performed in vivo experiments and purified cytochrome b_5, in addition to participation in the interpretation of the results. D. T. generated the pREP4-groESL_b5 vector, performed in vitro experiments, and purified bCPR$_{-27}$. M. C. H. performed and interpreted the docking simulations. F. H. and R. B. designed the study, participated in the interpretation of the results and manuscript drafting.

ORCID

Simone Brixius-Anderko http://orcid.org/0000-0002-3036-9285
Frank Hannemann http://orcid.org/0000-0001-7991-9033
Rita Bernhardt http://orcid.org/0000-0003-0961-7755

REFERENCES

Attardi, B. J., Zeleznik, A., Simhan, H., Chiao, J. P., Mattison, D. R., & Caritis, S. N. (2007). Comparison of progesterone and glucocorticoid receptor binding and stimulation of gene expression by progesterone, 17-alpha hydroxyprogesterone caproate, and related progestins. *American Journal of Obstetrics and Gynecology*, 197, 599–599.e7. https://doi.org/10.1016/j.ajog.2007.05.024

Bart, A. G., & Scott, E. E. (2017). Structural and functional effects of cytochrome b5 interactions with human cytochrome P450 enzyme. *The Journal of Biological Chemistry*, 292, 20818–20833. https://doi.org/10.1074/jbc.RA117.000220

Bavetta, L. A., Bekhor, I., Shah, R., O'Day, P., & Nimni, M. (1962). Metabolic and anti-inflammatory properties of 6-methyl prednisolone alone and in combination with anabolic hormones. *Endocrinology*, 71, 221–226. https://doi.org/10.1210/endo-71-2-221

Bernhardt, R. (2006). Cytochromes P450 as versatile biocatalysts. *Journal of Biotechnology*, 124, 128–145. https://doi.org/10.1016/j.jbiotec.2006.01.026

Bernhardt, R., & Urlacher, V. B. (2014). Cytochromes P450 as promising catalysts for biotechnological application: Chances and limitations. *Applied Microbiology and Biotechnology*, 98, 6185–6203. https://doi.org/10.1007/s00253-014-5767-7

Boland, E. W. (1961). Antirheumatic potency of chemically modified adrenocortical steroids. *American Journal of Medicine*, 31, 581–590. https://doi.org/10.1016/0002-9343(61)90142-5

Bridges, A., Gruenke, L., Chang, Y. T., Vakser, I. A., Loew, G., & Waskell, L. (1998). Identification of the binding site on cytochrome P450 2B4 for cytochrome b_5 and cytochrome P450 reductase. *Journal of Biological Chemistry*, 273, 17036–17049. https://doi.org/10.1074/jbc.273.27.17036

Brixius-Anderko, S., Schiffer, L., Hannemann, F., Janocha, B., & Bernhardt, R. (2015). A CYP21A2 based whole-cell system in *Escherichia coli* for the biotechnological production of premedrol. *Microbial Cell Factories*, 14, 1–14. https://doi.org/10.1186/s12934-015-0333-2

Bureik, M., & Bernhardt, R. (2007). Steroid hydroxylation: Microbial steroid biotransformations using cytochrome P450 enzymes. *Modern Biooxidation: Enzymes, Reactions and Applications*, 155–176. https://doi.org/10.1002/9783527611522.ch6

Cole, P. A. (1996). Chaperone-assisted protein expression. *Structure*, 4, 239–242. https://doi.org/10.1016/S0969-2126(96)00028-7

Diederich, S., Eigendorff, E., Burkhardt, P., Quinkler, M., Bumke-vogt, C., Rochel, M., ... Ba, V. (2015). *Important Pharmacokinetic Determinant for the Activity of Synthetic Mineralo- and Glucocorticoids*, 87, 5695–5701. https://doi.org/10.1210/jc.2002-020970

Edwards, V. H. (1970). The influence of high substrate concentrations on microbial kinetics. *Biotechnology and Bioengineering*, 12, 679–712. https://doi.org/10.1002/bit.260120504

Eisenberg, D. (1984). Three-dimensional structure of membrane and surface proteins. *Annual Review of Biochemistry*, 53, 595–623. https://doi.org/10.1146/annurev.bi.53.070184.003115

Farman, N., & Rafestin-Oblin, M.-E. (2017). Multiple aspects of mineralocorticoid selectivity. *American Journal of Physiology—Cell Physiology*, 280, F181–F192. https://doi.org/10.1152/ajprenal.2001.280.2.f181

Gasteiger, E., Hoogland, C., Gattiker, A., Duvaud, S., Wilkins, M.R., Appel, R.D., & Bairoch, A. (2005). Protein identification and analysis tools on the ExPASy server, *Proteomics protocols handbook* (pp. 571–607). Humana Press.

Gilep, A. A., Guryev, O. L., Usanov, S. A., & Estabrook, R. W. (2001). An enzymatically active chimeric protein containing the hydrophilic form of NADPH-cytochrome P450 reductase fused to the membrane-binding domain of cytochrome b_5. *Biochemical and Biophysical Research Communications*, 284, 937–941. https://doi.org/10.1006/bbrc.2001.5075

Gorsky, L. D., & Coon, M. J. (1986). Effects of conditions for reconstitution with cytochrome b_5 on the formation of products in cytochrome P-450-catalyzed reactions. *Drug Metabolism and Disposition: The Biological Fate of Chemicals*, 14, 89–96.

Gruenke, L. D., Konopka, K., Cadieu, M., & Waskell, L. (1995). The stoichiometry of the cytochrome P-450-catalyzed metabolism of methoxyflurane and benzphetamine in the presence and absence of cytochrome b_5. *Journal of Biological Chemistry*, 270, 24707–24718. https://doi.org/10.1074/jbc.270.42.24707

Guex, N., & Peitsch, M. C. (1997). SWISS-MODEL and the Swiss-PdbViewer: An environment for comparative protein modeling. *Electrophoresis*, 18, 2714–2723. https://doi.org/10.1002/elps.1150181505

Henzen, C. (2003). Therapie mit Glukokortikoiden: Risiken und Nebenwirkungen. *Schweizerisches Medizin-Forum*, 3(19), 442–446. https://doi.org/10.4414/smf.2003.04866

Hlavica, P., Schulze, J., & Lewis, D. F. V. (2003). Functional interaction of cytochrome P450 with its redox partners: A critical assessment and update of the topology of predicted contact regions. *Journal of Inorganic Biochemistry*, 96, 279–297. https://doi.org/10.1016/S0162-0134(03)00152-1

Huey, R., Morris, G. M., Olson, A. J., & Goodsell, D. S. (2007). Software news and update. A semiempirical free energy force field with charge-based desolvation. *Journal of Computational Chemistry*, 28(6), 1145–1152. https://doi.org/10.1002/jcc

Ikeda, R. A., Ligman, C. M., & Warshamana, S. (1992). T7 promoter contacts essential for promoter activity in vivo. *Nucleic Acids Research*, 20, 2517–2524. https://doi.org/10.1093/nar/20.10.2517

Imai, Y., & Sato, R. (1977). The roles of cytochrome b_5 in a reconstituted N-demethylase system containing cytochrome P-450. *Biochemical and Biophysical Research Communications*, 75, 420–426. https://doi.org/10.1016/0006-291X(77)91059-2

Janocha, S., & Bernhardt, R. (2013). Design and characterization of an efficient CYP105A1-based whole-cell biocatalyst for the conversion of resin acid diterpenoids in permeabilized *Escherichia coli*. *Applied Microbiology and Biotechnology*, 97(17), 7639–7649. https://doi.org/10.1007/s00253-013-5008-5

Kadmiel, M., & Cidlowski, J. A. (2013). Glucocorticoid receptor signaling in health and disease. *Trends in Pharmacological Sciences*, 34, 518–530. https://doi.org/10.1016/j.tips.2013.07.003

Katagiri, M., Kagawa, N., & Waterman, M. R. (1995). The role of cytochrome b_5 in the biosynthesis of androgens by human P450c17. *Archives of Biochemistry and Biophysics*, 317, 343–347. https://doi.org/10.1006/abbi.1995.1173

Klymiuk, M. C., Neunzig, J., Bernhardt, R., Sánchez-guijo, A., Hartmann, M. F., & Wudy, S. A. (2017). Journal of steroid biochemistry and molecular biology efficiency of the sulfate pathway in comparison to the Δ4- and Δ5-pathway of steroidogenesis in the porcine testis. *Journal of Steroid Biochemistry and Molecular Biology*, 0–1. https://doi.org/10.1016/j.jsbmb.2017.10.017

Koechlin, B. A., Kritchevsky, T. H., & Gallagher, T. (1951). Partial synthesis of compounds related to adrenal cortical hormones. XV. 17α, 21-dihydroxy-Δ4-pregnene-3, 20-dione (Reichstein's "Substance S"). *Journal of the American Chemical Society*, 73, 189–194.

Kyte, J., & Doolittle, R. F. (1982). A simple method for displaying the hydropathic character of a protein. *Journal of Molecular Biology*, 157, 105–132. https://doi.org/10.1016/0022-2836(82)90515-0

Lin, Y., Lu, P., Tang, C., Mei, Q., Sandig, G., Rodrigues, A. D., ... Shou, M. (2001). Substrate inhibition kinetics for cytochrome P450-catalyzed reactions. *Drug Metabolism and Disposition: The Biological Fate of Chemicals*, 29, 368–374.

Lu, A. Y., West, S. B., Vore, M., Ryan, D., & Levin, W. (1974). Role of cytochrome b_5 in hydroxylation by a reconstituted cytochrome P-450-containing system. *Journal of Biological Chemistry*, 249, 6701–6709.

Masters, B. S. S. (2005). The journey from NADPH-cytochrome P450 oxidoreductase to nitric oxide synthases. *Biochemical and Biophysical Research Communications*, 338, 507–519. https://doi.org/10.1016/j.bbrc.2005.09.165

McMaster, A., & Ray, D. W. (2008). Drug Insight: Selective agonists and antagonists of the glucocorticoid receptor. Nature clinical practice. *Endocrinology & Metabolism*, 4, 91–101. https://doi.org/10.1038/ncpendmet0745

Migita, C. T., Togashi, S., Minakawa, M., Zhang, X., & Yoshida, T. (2005). Evidence for the hydrophobic cavity of heme oxygenase-1 to be a CO-trapping site. *Biochemical and Biophysical Research Communications*, 338, 584–589. https://doi.org/10.1016/j.bbrc.2005.08.045

Miller, W. L. (2005). Minireview: Regulation of steroidogenesis by electron transfer. *Endocrinology*, 146, 2544–2550. https://doi.org/10.1210/en.2005-0096

Miroux, B., & Walker, J. E. (1996). Over-production of proteins in *Escherichia coli*: Mutant hosts that allow synthesis of some membrane proteins and globular proteins at high levels. *Journal of Molecular Biology*, 260(3), 289–298.

Morgan, E. T., & Coon, M. J. (1984). Effects of cytochrome b_5 on cytochrome P-450-catalyzed reactions. Studies with manganese-substituted cytochrome b_5. *Drug Metabolism and Disposition*, 12, 358–364.

Morris, G. M., Goodsell, D. S., Halliday, R. S., Huey, R., Hart, W. E., Belew, R. K., ... Al, M. E. T. (1998). Automated docking using a Lamarckian

Genetic Algorithm and an empirical binding free energy function. *Journal of Computational Chemistry*, 19, 1639–1662.

Mulrooney, S. B., & Waskell, L. (2000). High-level expression in *Escherichia coli* and purification of the membrane-bound form of cytochrome b_5. *Protein Expression and Purification*, 19, 173–178. https://doi.org/10.1006/prep.2000.1228

Neunzig, J., Milhim, M., Schiffer, L., Khatri, Y., Zapp, J., Sánchez-Guijo, A., ... Bernhardt, R. (2017). The steroid metabolite 16(β)-OH-androstenedione generated by CYP21A2 serves as a substrate for CYP19A1. *Journal of Steroid Biochemistry and Molecular Biology*, 167, 182–191. https://doi.org/10.1016/J.JSBMB.2017.01.002

Neunzig, J., Sánchez-Guijo, A., Mosa, A., Hartmann, M. F., Geyer, J., Wudy, S. A., & Bernhardt, R. (2014). A steroidogenic pathway for sulfonated steroids: The metabolism of pregnenolone sulfate. *Journal of Steroid Biochemistry and Molecular Biology*, 144, 324–333. https://doi.org/10.1016/j.jsbmb.2014.07.005

Nishihara, K., Kanemori, M., Kitagawa, M., & Yura, T. (1998). Chaperone coexpression plasmids: Differential and synergistic roles of DnaK-DnaJ-GrpE and GroEL-GroES in assisting folding of an allergen of Japanese cedar pollen Cryj2, in *Escherichia coli*. *Applied and Environmental Microbiology*, 64(5), 1694–1699.

Omura, T., & Sato, R. (1964). The carbon of liver microsomes. *Journal of Biological Chemistry*, 239, 2370–2378.

Sagadin, T., Riehm, J. L., Milhim, M., Hutter, M. C., & Bernhardt, R. (2018). Binding modes of CYP106A2 redox partners determine differences in progesterone hydroxylation product patterns. *Communications Biology*, 1(1), 199. https://doi.org/10.1038/s42003-018-0104-9

Sandee, D., & Miller, W. L. (2011). High-yield expression of a catalytically active membrane-bound protein: Human P450 oxidoreductase. *Endocrinology*, 152, 2904–2908. https://doi.org/10.1210/en.2011-0230

Sanner, M. F. (1999). Python: A programming language for software integration and development. *Journal of Molecular Graphics & Modelling*, 17(1), 57–61.

Schenkman, J. B., & Jansson, I. (2003). The many roles of cytochrome b_5. *Pharmacology and Therapeutics*, 97, 139–152. https://doi.org/10.1016/S0163-7258(02)00327-3

Schenkman, J. B., Jansson, I., & Robie-Suh, K. M. (1976). The many roles of cytochrome b_5 in hepatic microsomes. *Life Sciences*, 19, 611–623. https://doi.org/10.1016/0024-3205(76)90156-9

Schiffer, L., Brixius-Anderko, S., Hannemann, F., Zapp, J., Neunzig, J., Thevis, M., & Bernhardt, R. (2016). Metabolism of oral turinabol by human steroid hormone-synthesizing cytochrome P450 Enzymes. *Drug Metabolism and Disposition: The Biological Fate of Chemicals*, 44, 227–237. https://doi.org/10.1124/dmd.115.066829

Schäcke, H. (2002). Mechanisms involved in the side effects of glucocorticoids. *Pharmacology and Therapeutics*, 96, 23–43. https://doi.org/10.1016/S0163-7258(02)00297-8

Schäcke, H., Schottelius, A., Döcke, W. D., Strehlke, P., Jaroch, S., Schmees, N., ... A. K. (2004). Dissociation of transactivation from transrepression by a selective glucocorticoid receptor agonist leads to separation of therapeutic effects from side effects. *Proceedings of the National Academy of Sciences*, 101, 227–232. https://doi.org/10.1073/pnas.0300372101

Shen, A. L., Porter, T. D., Wilson, T. E., & Kasper, C. B. (1989). Structural analysis of the FMN binding domain of NADPH-cytochrome P-450 oxidoreductase by site-directed mutagenesis. *Journal of Biological Chemistry*, 264, 7584–7589.

Urlacher, V. B., & Girhard, M. (2012). Cytochrome P450 monooxygenases: An update on perspectives for synthetic application. *Trends in Biotechnology*, 30, 26–36. https://doi.org/10.1016/j.tibtech.2011.06.012

Venkateswarlu, K., Lamb, D. C., Kelly, D. E., Manning, N. J., & Kelly, S. L. (1998). The N-terminal membrane domain of yeast NADPH-cytochrome P450 (CYP) oxidoreductase is not required for catalytic activity in sterol biosynthesis or in reconstitution of CYP activity. *Journal of Biological Chemistry*, 273, 4492–4496. https://doi.org/10.1074/jbc.273.8.4492

Vergères, G., & Waskell, L. (1995). Cytochrome b_5, its functions, structure and membrane topology. *Biochimie*, 77, 604–620. https://doi.org/10.1016/0300-9084(96)88176-4

Vermillion, Janice, L., & Coon, M. (1978). Purified liver microsomal NADPH-cytochrome P-450 reductase. Spectral characterization of oxidation-reduction states. *Journal of Biological Chemistry*, 253(8), 2694–2704.

Wade, R. C., Winn, P. J., Schlichting, I., & Sudarko (2004). A survey of active site access channels in cytochromes P450. *Journal of Inorganic Biochemistry*, 98, 1175–1182. https://doi.org/10.1016/j.jinorgbio.2004.02.007

Wang, C., Pallan, P. S., Zhang, W., Lei, L., Yoshimoto, F. K., Waterman, M. R., ... Guengerich, X. F. P. (2017). Functional analysis of human cytochrome P450 21A2 variants involved in congenital adrenal hyperplasia. *Journal of Biological Chemistry*, 450, 10767–10778. https://doi.org/10.1074/jbc.M117.792465

Zhao, B., Lei, L., Kagawa, N., Sundaramoorthy, M., Banerjee, S., Nagy, L. D., ... Waterman, M. R. (2012). Three-dimensional structure of steroid 21-hydroxylase (cytochrome P450 21A2) with two substrates reveals locations of disease-associated variants. *Journal of Biological Chemistry*, 287, 10613–10622. https://doi.org/10.1074/jbc.M111.323501

SUPPORTING INFORMATION

Additional supporting information may be found online in the Supporting Information section.